Dethlefs, A.; Roos, A.; dos Santos, J.F.; Wimmer, G.:

Hybrid Friction Diffusion Bonding of Aluminium Tube-to-Tube-Sheet Connections in Coil-Wound Heat Exchangers

In: Materials and Design (2014) Elsevier

DOI: 10.1016/j.matdes.2014.03.049

Hybrid Friction Diffusion Bonding of Aluminium Tube-to-Tube-Sheet Connections in Coil-Wound Heat Exchangers[1]

A. Dethlefs [a, 2], A. Roos [a, 3], J. F. dos Santos [a], G. Wimmer [b]

(a) Helmholtz-Zentrum Geesthacht

Centre for Materials and Coastal Research,

Institute of Materials Research,

Materials Mechanics,

Solid State Joining Processes,

Max-Planck-Straße 1, 21502 Geesthacht, Germany

(b) Linde AG,

Engineering Division,

Werk Schalchen,

Carl-von-Linde-Straße 15, 83342 Tacherting, Germany

Abstract

The present study presents and evaluates an application of a new solid-state bonding process, hybrid friction diffusion bonding (HFDB). HFDB is used to fabricate tube-to-tube-sheet connections for aluminium coil-wound heat exchangers. An industry-applicable process variant is developed, and its feasibility is demonstrated by gas leak tightness tests and tensile pull-out tests. The joints meet the requirements of industrial

[1] This document is a collaborative effort.

[2] Present address: Institute for Machine Tools and Factory Management, Technical University Berlin, Chair of Machine Tools and Manufacturing Technology, Straße des 17. Juni 135, 10623 Berlin, Germany

[3] Corresponding Author

Email addresses: **arne.dethlefs@iwf.tu-berlin.de** (A. Dethlefs),
arne.roos@hzg.de (A. Roos),
jorge.dos.santos@hzg.de (J. F. dos Santos)
georg.wimmer@linde-le.com (G. Wimmer)

applications. Furthermore, the process is characterised by the thermal field development in the weld area and the applied process forces. The microstructure of the joint is investigated, and dynamic recrystallization is assumed to be the primary grain refinement mechanism in the thermo-mechanically affected zone.

Keywords

Joining; welding; diffusion; bonding; heat exchanger; aluminium

1 Introduction

Heat exchangers are commonly used for efficient heat transfer between different media and are widely used in industrial applications, such as petroleum refineries, power plants, and natural gas processing units. Coil-wound heat exchangers are typically used to create liquefied natural gas (LNG), as shown in Figure 1(a). For this low-temperature application, the heat exchangers are typically made from 5xxx series aluminium alloys. The fabrication of aluminium coil-wound heat exchangers presents several challenges, one of which is joining the tubes to the tube sheet, as shown in Figure 1(b).

Hybrid friction diffusion bonding (HFDB) is a solid-state bonding process that was developed and patented by Helmholtz-Zentrum Geesthacht GmbH (HZG) and first described by Roos [1] [2]. HFDB can bond similar and dissimilar materials using a combined friction and diffusion process. This process was originally developed to join thin sheet metals and foils (up to 1 mm in thickness). A friction-based heat input on the surface of the workpieces accompanied by certain deformations activates diffusion processes over the contact surface of the materials to be joined and thus creates a metallic bond.

HFDB has been selected as a viable alternative to the currently used joining processes due to its robustness and efficiency as a mechanical joining process.
In this work, the new HFDB process is adapted to join tube-to-tube-sheet connections in coil-wound heat exchangers. The dimensions of the tubes and tube sheets are noted in Figure 2(a). A special tool was designed and manufactured from hot working steel, which is commonly used as tool material in solid-state joining. The tool consists of the friction surface shown in Figure 2(a1) and a conical feature shown in Figure 2(a2) to apply friction to the inner side of the tube.

Before the actual joining process, the tube and tube sheet are pressed against each other using a conical tube expander to hold the workpieces in place. The pressing is performed such that an excess tube length of 1 mm is created, which protrudes out over the upper surface of the tube sheet.

The tool is rotated at a speed of n_T in the joining process. A predefined axial force F_P is then applied. Figures 2(b) and 2(c) illustrate that the joining process can be divided into two phases. During the insertion phase, only the conical feature is in contact with the inner side of the tube. The applied friction generates heat, and the tube material in the contact zone between the conical feature and tube is plasticised. Furthermore, the oversized conical feature exerts significant pressure on the contact zone and causes plastic deformation of the workpiece in the weld area. Both the conical feature and friction surface are in contact with the workpiece during the welding phase. Full contact between the tool and workpiece results in a high heat input that, in addition to the applied pressure, joins the tube and tube sheet due to activating diffusion

processes in the contact zone between the tube and tube sheet. Finally, the tool is retracted after a predefined welding time.

In this work, tubes and tube sheet dummies were used as workpieces to represent actual tube-to-tube-sheet connections, as shown in Figure 2(d).

The objective of the joint project between HZG and Linde AG was to investigate the fundamentals and feasibility of HFDB for efficiently joining tubes to tube sheets. The primary demands posed for a tube-to-tube-sheet joint are leak tightness against helium and a tensile strength of 80% or greater of the base material (BM) strength. These demands are to be met through a robust and cost-effective process. This paper investigates the basic process principles, such as the temperature and deformation influence on the bond and the microstructure of the bond.

2 Experimental Procedures and Materials

In accordance with the materials used in coil-wound heat exchangers for cryogenic applications, aluminium alloys solid solution strengthened alloys of the 5xxx series were used for the tube sheet dummies and tubes, respectively. Table 1 presents the chemical composition of the two alloys. Figure 3 presents the microstructure of the two materials. The 5xxx series alloy, as used in this work for the tube sheet dummies, is a drawn material with the typical flattened grain structure in the drawing direction. The black indicators in the microstructure represent second-phase particles, identified as intermetallic compounds, such as Mn, Fe, Cr, Al_6, Mg_2Si, and Mg_5Al [3]. These second-phase particles are the nuclei that are essential for recrystallization during hot

deformation [4]. The 5xxx series alloy used for the tubes presents the typical structure of an annealed aluminium alloy with equiaxed grains.

All experiments described in this work were performed on a Tricept 805 5-axis parallel kinematic robot in a tripod configuration currently in supply from PKM-Tricept in Pamplona, Spain. The handling system is equipped with a HZG developed force control unit to apply the predefined axial process forces.

Radial forces were measured on the workpiece side with Kistler 3-axis piezoelectric sensors to calculate the torque applied during the process. Temperature data were recorded with type K Cr-Ni thermocouples, which were inserted in the tube sheet dummy at distances of 0.5 and 1 mm from the tube, as shown in Figure 6. Microscopic analysis was performed on cross-sections of the workpiece samples. The samples underwent metallographic grinding, polishing, and etching and were analysed under polarised light with a light optical microscope.

Tensile pull-out tests were conducted for mechanical characterisation, where the tubes were pulled out of the tube sheet dummies with a conventional tensile testing machine, as shown in Figure 4. The pull-out tests were performed according to an in-house standard of Linde AG. Helium leak tightness tests were performed with welded samples in accordance with DIN EN 1779:1999 [5]. Helium leak tightness tests can detect leak rates as small as 10^{-9} mbar·l/s.

3 Results and Discussion

3.1 Process Development

The parameters that govern the process could be estimated from the initial HFDB tests. The following parameters were identified:

- rotational speed of the tool
- applied axial process force
- welding time
- excess tube length
- angle of the conical feature on the tool
- surface roughness of the tube in the weld area

These parameters were evaluated in a series of experiments that were systematically planned and conducted using design of experiments, namely, a partial factorial and full factorial scheme based on the Design of Experiments (DoE) approach [7]. The process was evaluated based on the achieved pull-out strength, gas leak tightness, and microstructural quality of the weld area. Certain challenges had to be overcome in the process development, which are described below.

The friction between the conical feature of the tool and the inside of the tube during the insertion of the tool is an important factor. The torque, M_z, imposed on the workpiece by the tool is directly related to the friction, which was found to be crucial to the stability of the process. Poor plastification of the tube material during the insertion phase was observed to lead to a high torque at the transition between the insertion and welding phase. This high torque can cause the tool to become caught in the workpiece due to a lack of power of the spindle drive. Furthermore, vibrations can be caused by torque peaks, leading to process instability and, in some cases, tube

damage. These complications were traced back to the process force being applied in a step-like manner. The issue was solved by introducing a ramp-like process force. Figure 5 presents the torque, Mz, measured in two HFDB joints with the two types of process forces applied. A smoother tool entry can be achieved by applying force ramps (dashed line in Figure 5 (a)). The resulting measured torque peaks are less than 20 Nm as shown in Figure 5 (b) (grey graph), and the average torque during the welding phase is approximately 5 Nm. The difference from the step-like application of the process force (dotted lines in Figure 5 (a)) is clear. As shown in Figure 5 (b), a resulting peak torque of 34 Nm is measured. A force application with two ramps leading up to the maximum process force, which is 2,000 N in this case, was considered suitable to achieve a robust process (see Figure 5a). Furthermore, higher rotational speeds of the tool and relatively small angles of the conical feature have been shown to improve the process stability.

The process temperatures were measured in the tube sheet dummies close to the weld area at distances of 0.5 and 1 mm from the outside of the tube, as shown in Figure 6. As expected, the temperature is greater at the measurement point closer to the weld area. Nevertheless, the temperatures at both measurement points are almost equal toward the end of the welding phase.

The two phases of the process, insertion and welding, and the application of the force ramps affect the heating rate. The temperature increases gradually during tool insertion, where the temperature peaks correspond with the torque peaks measured during this phase. The temperatures increases rapidly to greater than 400°C upon application of the second force ramp and then stabilise with a declining increase

during the welding phase. The maximum temperature reached was approximately 520°C.

Temperatures of approximately 500°C during the welding phase proved to be sufficient for good plastification and thus for bonding. These temperatures can only be reached if the workpiece is slowly heated during the insertion phase. For this reason, a slow insertion of the tool is favourable in terms of the necessary heat input. In theory, a higher energy input, i.e., a higher rotational speed of the tool, will lead to higher temperatures and thus better plastification. For the HFDB application discussed here, this relationship holds for the insertion phase. Nevertheless, Roos [2] has demonstrated that excessive temperatures in the workpiece will not lead to a better bond because a layer of molten material forms around the tool, where the stick condition transforms into a slip condition that creates a polishing effect between the tool and the material to be bonded. An improved process strategy can be derived from the investigation of the process temperatures: high rotational speeds during the insertion phase and moderate speeds, as used in the experiments, during the welding phase.

3.2 Microstructure of the joint

The typical microstructure of a HFDB tube-to-tube-sheet connection can be divided into two zones, a thermo mechanically affected zone (TMAZ) and a heat-affected zone (HAZ), as shown in Figure 7. Both zones stretch out over the tube and tube sheet. The joint line cannot be observed using optical microscopy because the bonding mechanism is based on diffusion.

Figure 8 presents the microstructure of a HFDB tube-to-tube-sheet joint. The typical structure of the BM of the tube sheet with large grains stretched in the drawing direction can be observed. The TMAZ features fine, equiaxed grains; the average grain size in this region is 21 µm. The primary grain refinement mechanism in this area is assumed to be dynamic recrystallization, as considered in studies on hot deformation in 5xxx series aluminium alloys [3][4][5]. Because temperatures in the weld area reached approximately 500-550°C, the HFDB can be compared with a high-strain-rate hot-deformation process. The HAZ, which is situated between the BM and TMAZ, exhibits a gradual grain enlargement. Furthermore, the shape gradually changes from equiaxed to elongated grains. If the grain refinement in the TMAZ is caused by dynamic recrystallization, as described above, it can be assumed that partially recrystallized grains dominate the microstructure of the HAZ.

Because temperatures reached 550°C in the weld area, it is apparent that the HAZ is also affected by the weld thermal cycle, which can cause changes in the material, although the microstructure does not change significantly due to a lack of deformation. Further examination is required to investigate the effects of the weld thermal cycle on the material.

The sizes of the HAZ and TMAZ and thus the size of the bonded area depend heavily on the process parameters. The depth of the affected zone, as marked in Figure 8, varied between 1 and 3 mm. Increasing the bond depth to more than 1 mm was one of the requirements from Linde AG for the investigation of the tube to tube-sheet HFDB welds.

Longer HFDB welding times as well as higher rotational speed and torque lead to higher energy input. Increasing the energy input from 15 kJ to 34 kJ increases the bond depth as shown in Figure 10 (grey dashed line). For these welds the joining geometry is not altered.

To overcome the necessity for even higher energy inputs a stand out of the tube above the weld area prior to welding is used to increase the strain in the weld area. The stand out has to be flattened by the tool during welding therefore increasing the strain rate in the weld area compared to the HFDB joints without tube stand out. As can be seen from Figure 10 (black dotted line) energy inputs of 30 kJ and 24 kJ coupled with a stand out of the tube of 1 mm increases the bond depth to more than 2 mm.

The above described observation is made throughout the HFDB joints investigated. Further systematic research is required due to the lack of statistically valid data.

A tube stand out that protrudes by approximately 1 mm had the best results.

3.3 Testing

3.3.1 Gas Leak Tightness

Overall, 23 HFDB tube-to-tube-sheet connection samples were tested for helium leak tightness. All samples exhibited a leak rate of less than 10^{-9} mbar·l/s, which is equal to an ideal sealing against gas leakage. Because all samples had the same result, it can be assumed that an extremely low error rate with respect to gas leak tightness can be achieved with HFDB in this particular application.

3.3.2 Mechanical Characterisation

Tensile pull-out tests were conducted with HFDB tube-to-tube-sheet connections joined at different rotational speeds. A tensile strength of 80% of the BM strength must be reached to meet the requirements for the industrial application. The tensile strength of the BM, e.g., tensile strength of the tube, is 217 MPa, and thus, a tensile pull-out strength of 174 MPa is the minimum value that must be reached.

Figure 9 presents the tensile pull-out strength for joints welded at different rotational speeds with the respective standard deviation compared to the strength of the BM. The requirement of 80% strength of the BM was met in all experiments. The best results were reached for rotational speeds of nT=1,500 min^{-1} and nT=1,800 min^{-1}; however, a correlation between the joint strength and rotational speed could not be established.

As shown by the example in Figure 11, all HFDB joints failed at approximately 3-5 mm below the actual weld area and TMAZ, where the bond was established. It can therefore be assumed that the actual bond can withstand even higher loads. The difference in the strength between BM and tested joints (see Figure 9) can be ascribed to the plastic deformation and thus the thinning of the tube walls due to the pre-process rolling, which is the primary reason why an actual correlation between the process parameters and mechanical strength of the bonds could not be established.

4 Conclusions

This study has presented and evaluated an application of the HFDB process. The following conclusions were obtained:

- A number of parameters control the process stability and joint quality, including rotational speed, axial force, welding time, excess tube length and tool geometry. The dimensions of the welded region are primarily defined by the rotational speed, process forces, and tool geometry.
- Process forces and process temperatures were investigated, and two phases, namely, the insertion and welding phases, were identified. For a stable, robust process, a gradual, slow increase in the process force during the insertion phase is favourable for the tool geometry used (i.e., ramping).
- The weld microstructure, as observed by optical microscopy, consisted of three zones: the TMAZ, the HAZ, and non-affected BM. The TMAZ undergoes significant mechanical deformation under temperature and is characterised by fine equiaxied grains. The HAZ is characterised by a gradual grain growth and an ill-defined boundary around the unaffected BM.
- The grain refinement in the TMAZ can be ascribed to dynamic recrystallisation based on the observed microstructure, process temperatures, and degree of deformation in the weld area.
- The mechanical and leak tightness tests displayed positive results. All samples exhibited a leak rate of less than 10^{-9} mbar·l/s. The pull-out strength of the tested samples was greater than 80% of the strength of the BM. A correlation between the joint strength and rotational speed could not be established.
- The requirements for the industrial application of the HFDB process on the fabrication of aluminium coil-wound heat exchangers were met.

References:

[1] Roos et al.: Process and device for producing a weldment between the surfaces of two flat workpieces with total running of the contacting surfaces of the friction stir tool into the surface of the second workpiece opposing the first workpiece. 2006, European Patent EP 1 769 877 B1.

[2] Roos: Grundlegende Untersuchung über ein neues Schweißverfahren namens HFDB (Hybrid Friction Diffusion Bonding). 2010, PhD Thesis, TU-Ilmenau.

[3] Hosseinipour et al.: An investigation into hot deformation of aluminum alloy 5083, Materials and Design 30(2): 319-322, 2009.

[4] Patankar et al.: Strain Rate Insensitive Plasticity in Aluminum Alloy 5083, Scripta Materialia, 38(8):1255-1261, 1998

[5] DIN EN 1779:1999

[6] Doherty et al.: Current issues in recrystallization: a review, Materials Science and Engineering A, 238(2):219-274, 1997

[7] Montgomery: Design and Analysis of Experiments, John Wiley & Sons, 2012

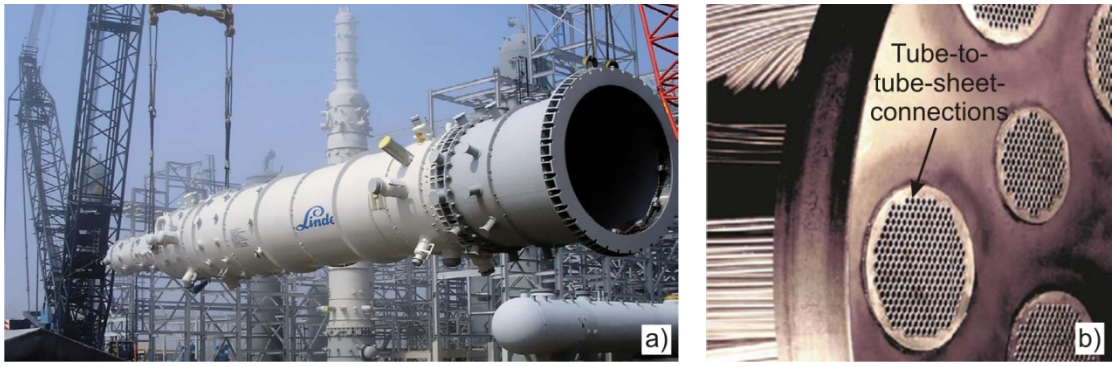

Figure 1 - a) Coil-wound heat exchanger for the liquefaction of natural gas; b) tube-to-tube sheet connections on a coil-wound heat exchanger. Source: Linde AG

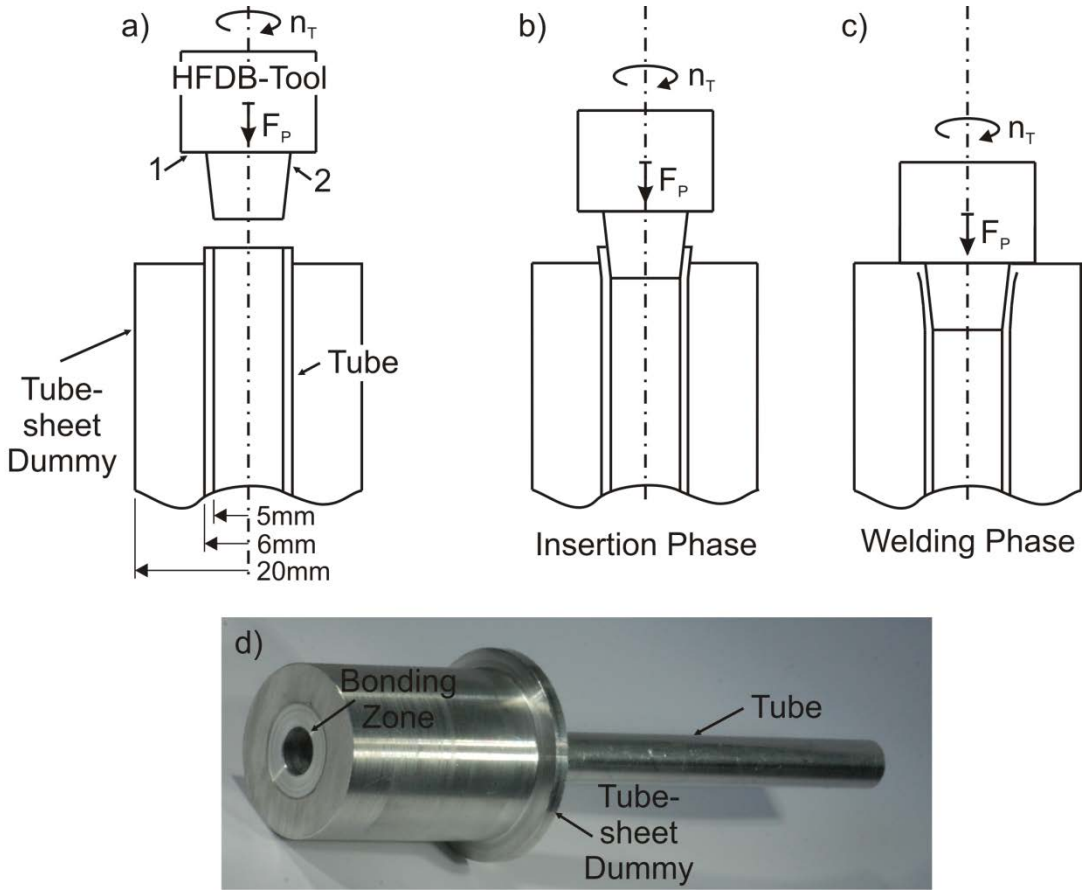

Figure 2 - a) Schematic overview of the HFDB tool and workpieces with (1) a friction surface and (2) a conical part; and HFDB process phases: insertion

phase b) and welding phase c); d) actual bonded specimen with bonding zone (left) of tube-sheet dummy and tube

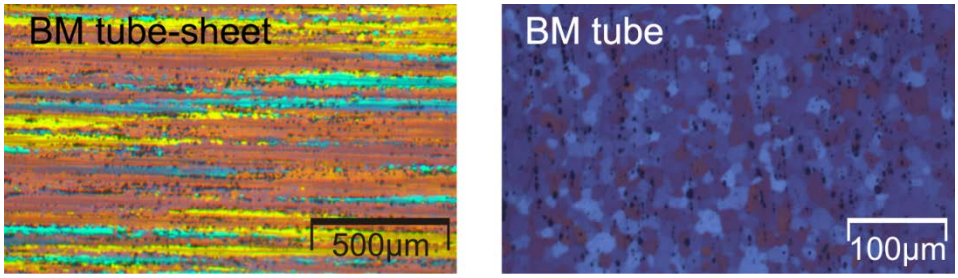

Figure 3 - BM microstructure of AA 5xxx tube-sheet dummy (left) and AA 5xxx tube (right)

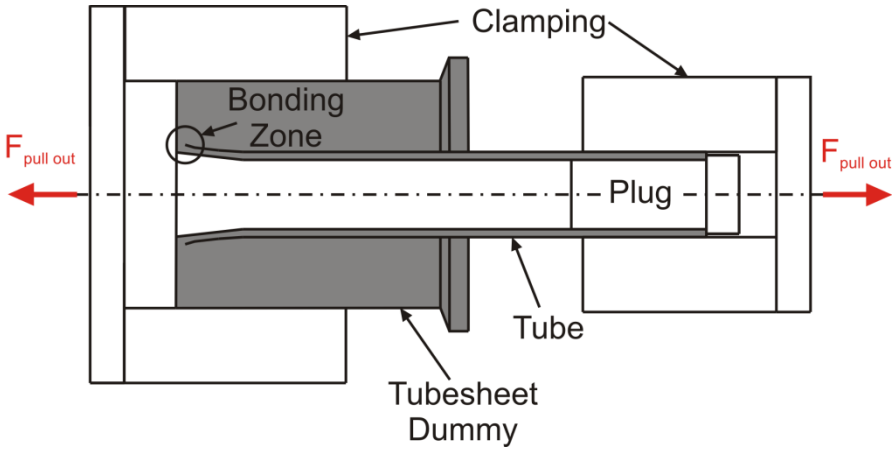

Figure 4 - Setup for the HFDB tube-sheet dummy to tube pull-out tests for evaluating the quasi-static strength of HFDB joints; the plug is inserted to prevent tube collapse during testing

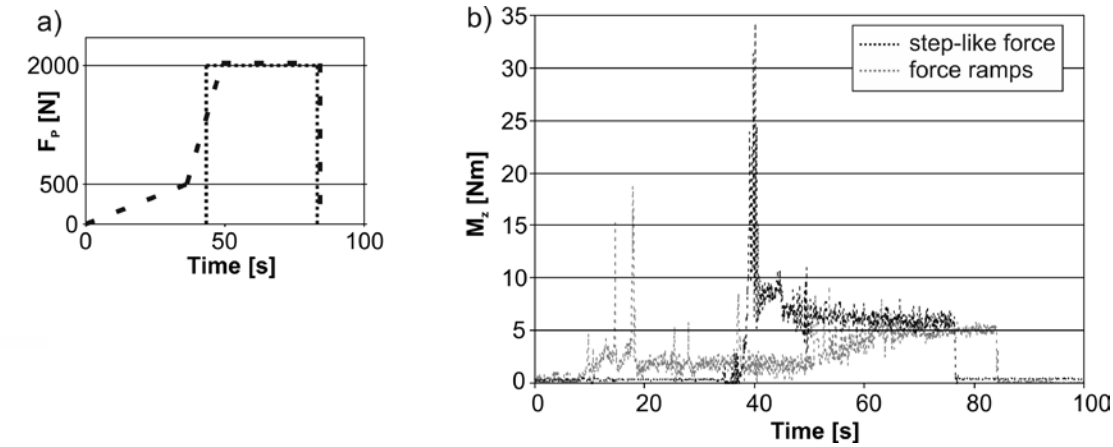

Figure 5 - a) applied step-like (dotted line) and ramp (dashed line) process forces b) measured torque during the HFDB process resulting from step-like (black graph) and ramp (grey graph) process forces

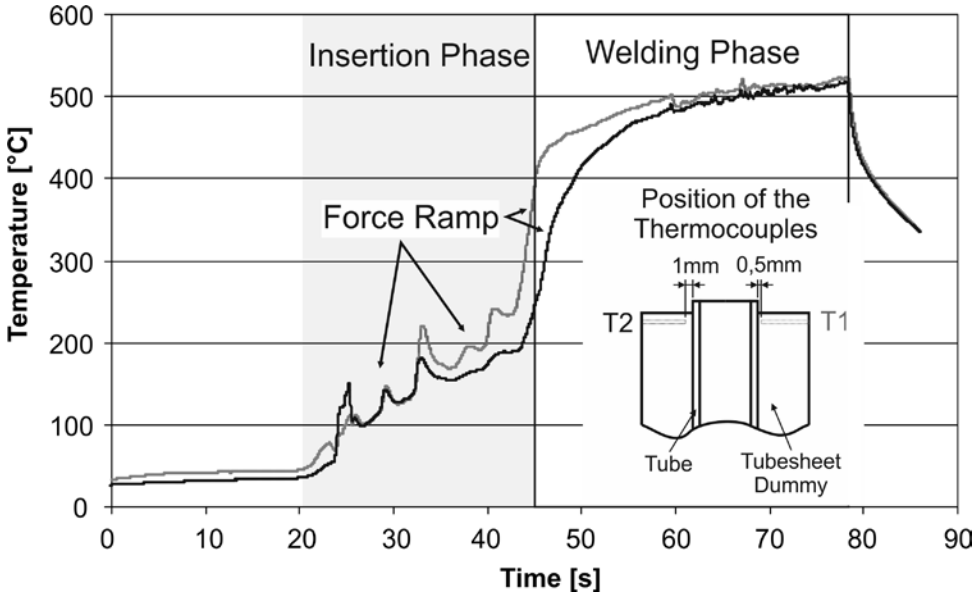

Figure 6 – Resulting HFDB process temperatures measured with thermocouples T1 (grey) and T2 (black) during the insertion and welding phases close to the weld area; the position of the thermocouples is schematically depicted in the graph

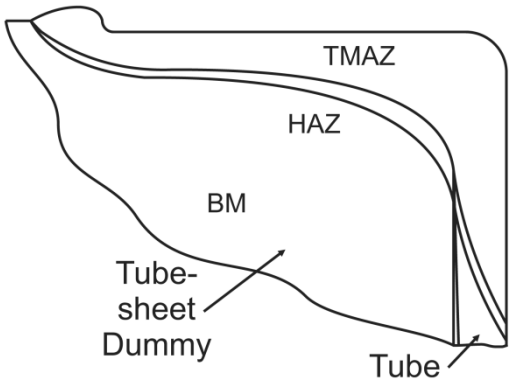

Figure 7 - Schematic overview of the microstructure in the HFDB tube-sheet dummy to the tube weld area with BM, HAZ, and TMAZ indicated

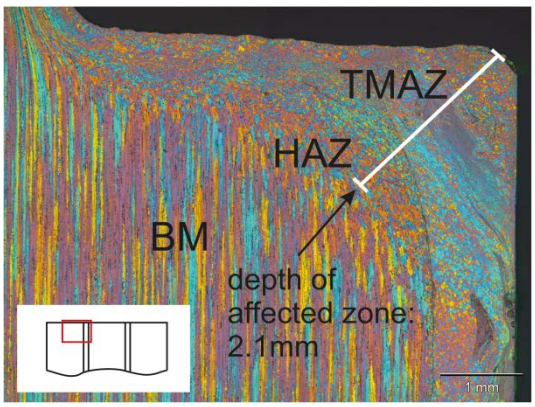

Figure 8 - Microstructure in the HFDB weld area from the BM of the tube sheet dummy through the HAZ to the TMAZ in the tube-sheet dummy / tube region

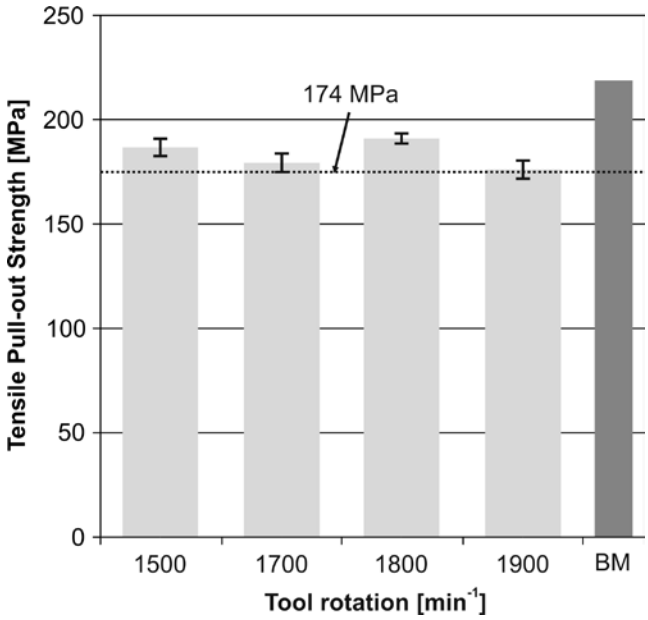

Figure 9 - Comparison of the HFDB tube-sheet dummy / tube pull-out test samples from HFDB welds at different rotational speeds with AA 5xxx tube BM tensile strength; 80 % tube BM tensile strength equals to 174 MPa

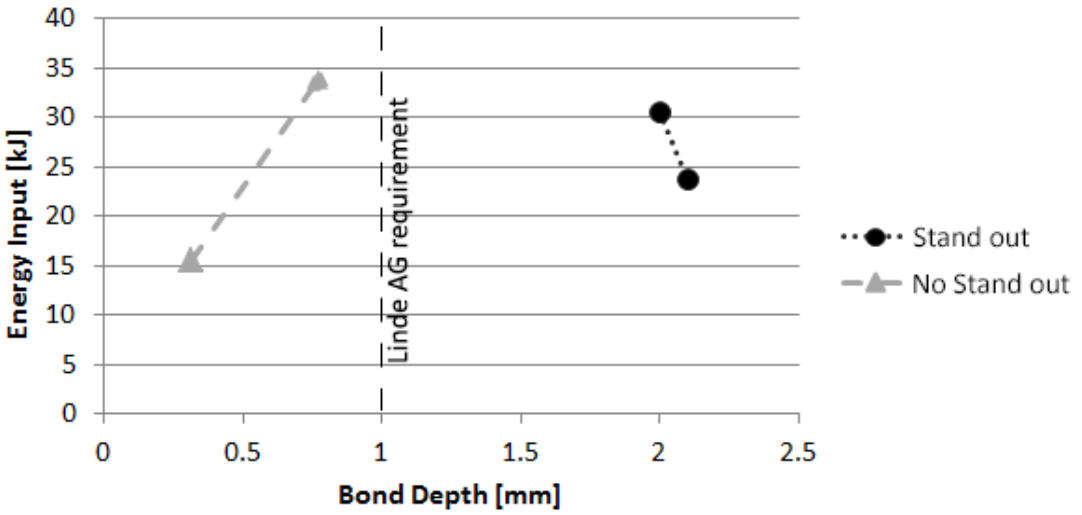

Figure 10 – Observation of energy input vs. bond depth of the HFDB tube-sheet dummy welds on the data of four screening welds; tube stand out selected to 1 mm; comparable energy input leads to higher bond depth for tube stand out welds

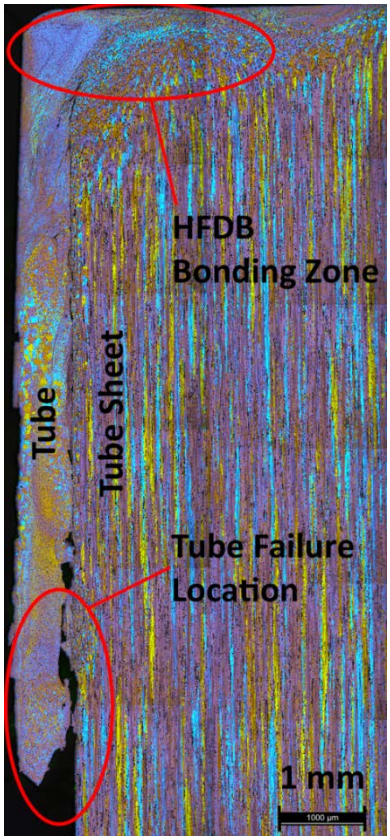

Figure 11 – Exemplary macro graphic overview of the tube failure location in a HFDB tube to tube-sheet dummy weld after pull-out test; failure outside HFDB bonding zone

Table 1 - Chemical composition of AA 5xxx solid solution strengthened alloys used, values in weight%

Material	Al	Mg	Mn	Fe	Si	Cr	Cu	Ti
AA 5xxx tube sheet dummy	94	4.5	0.64	0.32	0.19	0.068	0.041	0.023
AA 5xxx tube	95	1.7	0.52	0.18	0.13	0.001	0.001	0.01